Models of Ice and Dust Endmembers of the Southern Ice Dome on Mars. W. M. Calvin[1], S. F. A. Cartwright[2] and A. E. Covington[1,3], [1]Dept. of Geological Sciences, University of Nevada, Reno, NV 89557 (wcalvin@unr.edu), [2]Geological Sciences, University of Colorado, Boulder CO. [3]Dept. of Physics, University of Nevada, Reno.

Introduction: Mars has two polar ice domes, comprised primarily of water ice with small amounts of dust contamination. In the south, the highest albedo deposits (usually called the residual cap) sit only at the highest elevations and are carbon dioxide rather than water ice. Water ice has been observed along the margins of the bright residual CO_2 ice distinguished both by the difference in temperature and its unique spectral signature (e.g. [1-4], Fig. 1).

It has been assumed that the CO_2 and H_2O ices are stratigraphic layers with CO_2 on top of dirty water ice. However, the discovery of thick layers of CO_2 in the interior of the southern ice dome, interlayered with water ice, suggests more complicated relationships linked to past climate cycles that may (or may not) have a surface expression [7-9].

Recently Cartwright et al. [10] analyzed data from the Compact Reconnaissance Imaging Spectrometer for Mars (CRISM) and identified 21 spectral endmembers whose signatures range from CO_2 to H_2O only ices with a wide range of mixtures of the two and variable amounts of dust. Among the surprising results is that the signature of CO_2 ice is seen in dark materials away from the margin of the highest albedo CO_2 ice. This is even in late summer when seasonal ice has been removed. These results challenge the stratigraphic "layer cake" model based on the observed spatial distribution of various ice signatures. Compositional variability can help inform the history and evolution of the residual ice and its interaction with the atmosphere. To constrain ice abundances and grain sizes among these spectral endmembers we explore different mixture models.

Linear Mixing: As seen in some HiRISE images (e.g., Figure 2), carbon dioxide ice may be spatially isolated in patches that are below the CRISM resolution, and/or may form thin veneers over underlying dirty ice of either H_2O or CO_2 composition. Figure 2 identifies both outlier bright mesas and deposits that are subtly different in albedo in the darker regions, suggesting thin ice lingering in rough, dark terrain. Initially, the 21 endmembers were modeled as linear combinations of the three spectra that represent only CO_2, H_2O or dust [11]. However, using only three endmembers resulted in large residual errors. All 21 endmembers were successfully modeled using five components [11], two dominated by CO_2 ice, two by water ice and one dust endmember (Figure 3). The five components represent seasonal CO_2 ice (C1), residual CO_2 ice (C6), dust dominated surfaces (Dw1), and water ice with varying brightness and feature strength (W1, W3). This

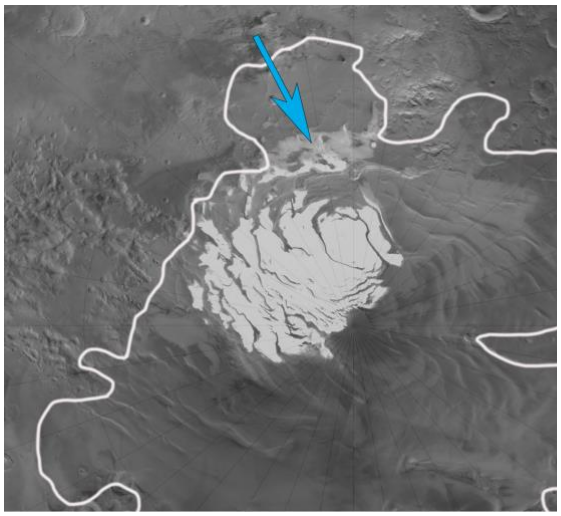

Figure 1: Mars Observer camera image of the south residual ice dome on Mars. The white outline identifies lower albedo, elevated materials that are relatively transparent to radar signals implying they are ice (after [5, 6]). The brightest materials are CO_2 ice and the blue arrow points to a region of intermediate brightness that is exposed H_2O ice.

suggests that at the 18m/pixel spatial scale of CRISM highest spatial resolution data, "geographic" or spatially segregated patches of various types of ice do a reasonable job of simulating typical surfaces that are observed. Our first goal in modeling all 21 endmembers is to understand the nature of these five relatively "pure" constituents.

Radiative Transfer Models: A range of radiative transfer models have been used to describe the intimate mixture of water and carbon dioxide ices expressed in the southern perennial high albedo deposits [e.g. 3, 14, 15]. We use the optical constants compiled from various sources by H. Kieffer [14, 16] and first attempted matches to the endmembers shown in Figure 3 using the Markov Chain Monte Carlo minimization of Lapotre et al. [17]. Unfortunately, that approach was not successful as all model fits are dominated by water ice with very low correlation coefficients. Even the most water ice rich endmembers are poorly modeled. We thus shifted to a simplified forward Hapke [18] model using two component mixtures (one ice and dust) as a starting point to explore the five primary constituents. Following [3] we note that the dust grain size does not strongly impact model fits. Starting grain sizes for both water and carbon dioxide ices were initially set to values from previous work [3,14,15].

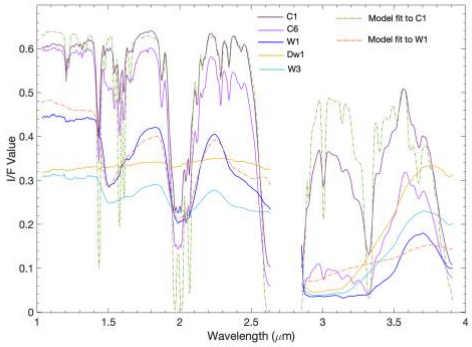

Figure 3: Spectra of five endmembers that were used in linear combination to model all 21 spectral endmembers identified by [10]. Reference numbers reflect usage in [10]. C=CO_2 dominant, W=H_2O dominant, Dw=dusty water ice. See text for discussion of endmembers and model fits.

Preliminary Results: Figure 3 shows 2 component fits for C1 and W1 endmembers. The C1 fit uses 97% CO_2 at a 2 mm grain size and dust at 2 μm. While the band depths of features near 2.3 μm fit well, the other features are too strong and the spectrum is too bright beyond 3 μm. The W1 fit uses 25% water at 60 μm and dust at 0.7 μm. The 1.5 and 2.0 μm water ice bands fit well, but the overall slope is off and the region beyond 3 μm doesn't fit at all. These initial models suggest the need to include water even in the CO_2 dominant endmembers, as well as temperature-sensitive H_2O coefficients to reproduce the feature near 1.65 μm. We also need to incorporate a better model for the dust to fit the longer wavelengths more accurately. We will present additional models at the meeting and are working to develop more detailed spectral inversions that include all three components.

References: [1] Titus et al. (2003) *Science*, *299*, 1048. [2] Bibring et al. (2004) *Nature*, *428*, 627. [3] Douté et al. (2007) *Planet Space Sci*, *55*, 113. [4] Piqueux et al. (2008) *JGR Planets*, DOI: 10.1029/2007je003055. [5] Tanaka et al. (2014) USGS SI Rep. 3292, DOI:10.3133/sim3292. [6] Khuller and Plaut (2021) *GRL*, doi: 10.1029/2021GL093631. [7] Philipps et al. (2011) *Science*, 332, 838, doi: 10.1126/ science.1203091 [8] Bierson et al. (2016) *GRL*, 43, doi:10.1002/2016GL068457. [9] Buhler et al. (2020) *Nature Astronomy*, *4*, 364, doi: 10.1038/s41550-019-0976-8. [10] Cartwright et al. (2022) *JGR Planets*, in press, 2022JE007372. [11] Cartwright, S. F.A. (2021) MS thesis, Univ Nev Reno. [12] Thomas et al. (2013) *Icarus*, *225*, doi:10.1016/j.icarus.2012.08.038. [13] www.uahirise.org. [14] Kieffer et al. (2000) *JGR 105(E4)*, 9653. [15] Hansen et al. (2005) *Planet Space Sci*, *53*, 1089. [16] H. H. Kieffer, personal communication to WMC. [17] Lapotre et al. (2017) *JGR-Planets*, *122*, 983, doi:10.1002/2016JE005248. [18] Hapke (1981) *JGR, 86(B4)*, 3039.

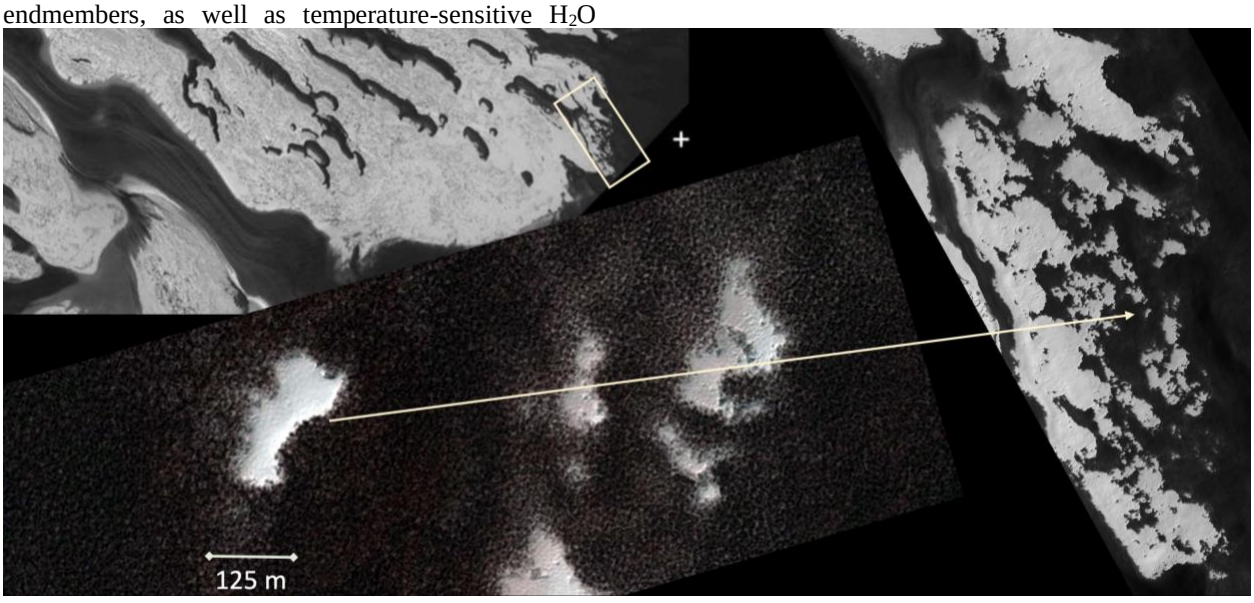

Figure 2: The upper left image shows the regional context (from [12]) of residual CO_2 ice at the Martian south pole in late summer (white cross is the geographic south pole, box is approximate location for the HiRISE image at the right). Image at right is a reduced scale version of HiRISE image ESP_023548_0900 [13]. Image at the lower left is a zoom in showing detail on bright mesas and surrounding terrain. The arrow points to the location in the full image. Note the patchy bright material that surrounds the mesas, which is inferred to be CO_2 ice over a dark water ice substrate. Scale bar is ~ 7 CRISM pixels wide.